

**PUBLISHED IN: ATMOSPHERIC MONITORING AND ASSESSMENT (2008/February)**

**DOI: 10.1007/s10661-008-0221-x**

**AVAILABLE AT: <http://dx.doi.org/10.1007/s10661-008-0221-x>**

## **SEASONAL DIFFERENCES IN SO<sub>2</sub> GROUND-LEVEL IMPACTS FROM A POWER PLANT PLUME ON COMPLEX TERRAIN**

*Palau, J.L. (1); Meliá, J. (2); Segarra, D. (2); Pérez-Landa, G. (1); Santa-Cruz, F. (1); Millán, M.M. (1)*

*(1) Fundación Centro de Estudios Ambientales del Mediterráneo (CEAM). [jlp@confluencia.biz](mailto:jlp@confluencia.biz)*

*C/ Charles R. Darwin, 14. 46980 Paterna (València). SPAIN.*

*(2) Universitat de València. Departamento de Termodinàmica. Burjassot (València). SPAIN.*

### **ABSTRACT**

The objective of this study is to describe the seasonal differences in SO<sub>2</sub> ground-level fumigations from a power plant situated on very complex terrain in the Iberian Peninsula within the Western Mediterranean Basin (WMB). The study area extends more than 80 kilometres around the power plant on very complex semi-arid terrain. Considering different plume-rise schemes, by experimentation and modelling this study attempts to characterise the seasonal differences in both the plume footprint 80 kilometres around the power plant and the turbulent regime (diurnal or nocturnal) driving the main contribution to the accumulated plume footprints at different distances from the power plant within a complex terrain region. Two markedly different SO<sub>2</sub> ground-level distributions around the power plant are presented for the typical summer and winter dispersive scenarios in the area. Simulations show that the SO<sub>2</sub> footprint of a plume being advected more than 450 metres above ground level in complex terrain is highly dependent on the prevailing meteorological conditions and on the mesoscale perturbations of the synoptic flows within the lower layers of the troposphere. The results obtained show how on complex terrain, despite seasonal meteorological differences and under stable dispersive conditions, the simulated mechanical turbulence leeward of the mountain ranges reproduces highly concentrated SO<sub>2</sub> fumigations on the ground more than 50 kilometres away from the power plant. Besides, under summer convective activity, plume fumigations have been successfully simulated less than 15 kilometres from the power plant. In conclusion, this study shows how measurements from air quality networks together with information obtained from atmospheric transport and diffusion models are able to characterise different transport scenarios. This is a clear advantage for the end-users and decision-makers who manage and optimise the regional air quality networks.

**Key-words:** Atmospheric dispersion, modelling, complex terrain, ground-level concentration, mesoscale, power plant, seasonal variability.

### **1. INTRODUCTION**

Monitoring systems designed to assess ground-level concentrations of anthropogenic emissions of air pollutants on complex terrain are seriously limited with respect to the spatial representativity of measurements from surface air quality networks (Fast et al., 1995; Fast and Darby, 2004). A general feature is the presence of very high gradients within a few kilometres, directly linked to terrain heterogeneities (Fast, 1995; Zaremba and Carroll, 1999); in this sense, the spatial representativity of the measurement data can be assessed by employing validated mesoscale models (COST-710, 1998; Palau et al., 2006) that take into account the terrain height variance within the simulated domain (Salvador et al.; 1999) and the meteorological interactions between the different scales (Palau et al., 2005).

Another critical aspect in the study of pollutant dispersion on complex terrain is the displacement between the mean direction of pollutant plumes aloft and their surface impact zones (vertical wind directional shear, Pooler and Niemeyer, 1971; Shiermeier, 1971; Millán et al. 1976, 1986, 1987; Palau 2003). Vertical wind directional shear can show important seasonal variations in frequency and intensity, due to interactions not only between synoptic flows and topographic channelling and/or decoupling of wind flows between the lower and the upper layers of the troposphere, but also between the general flow and the thermal winds that develop following a daily cycle (Millán et al. 1987, 2004). Thus, the seasonal differences in mesoscale forcings are expected to be associated with different distributions in the ground-level SO<sub>2</sub> concentrations.

These different “spatial distributions of the ground-level SO<sub>2</sub> concentration” are hereafter referred to as “plume footprints”.

Therefore, for a credible evaluation of the impacts of anthropogenic emissions from urban to regional scales, one needs to implement within numerical models all the spatial and temporal interactions between topography and atmosphere in the lower layers of the troposphere. In this paper, we describe seasonal differences in the plume footprint around a power plant situated on very complex terrain. The power plant selected, with a 343-meter-tall chimney, is located in the Northeast of the Iberian Peninsula (labelled APP in figure 1) and the SO<sub>2</sub> plume emitted is affected by mesoscale forcings of the wind flow (Palau et al. 2001; Pérez-Landa et al. 2002; Palau 2003, Palau et al. 2006). Previous studies in the area showed that Gaussian regulatory dispersion models cannot be applied under the most recurrent meteorological conditions because of the limitations assumed (Millán, 1987; Palau et al. 2001; Perez-Landa et al., 2002; Palau et al., 2004a). In summer, the development of the Iberian Thermal Low during the day forces the surface-wind flows to merge into several major convergence lines, which become landlocked to the main orographic features (Millán et al. 1992). In winter, advective conditions prevail and pollutant dispersion is driven by strong mechanical turbulence forced by topography, by strong ground-based radiative inversions during the night and by stratification of different stable layers over the different valleys in the area also at night (Palau, 2003).

The objective of this study is to describe the seasonal differences in SO<sub>2</sub> ground-level impacts from the Andorra Power Plant (APP) situated on very complex terrain in the Western Mediterranean Basin (WMB), within the Iberian Peninsula. The results presented are complementary to previous studies describing the atmospheric dispersion of the plume aloft emitted during the same field campaigns used in the study presented in this paper (Pérez-Landa et al. 2002, Palau et al. 2006). By experimentation and modelling, this study attempts to characterise the patterns observed in the ground-level impacts at distances from a few kilometres to more than 80 kilometres around the power plant under two recurrent and extreme meteorological situations representing typical summer and winter conditions.

In the paper we begin by describing the methodology used (section 2) and the meteorological conditions during the two field campaigns considered (section 3). Then, using different plume-rise schemes, we analyse the seasonal dependence on the plume footprint around the power plant. We also discuss seasonal differences in the turbulent regime (diurnal or nocturnal) that drives the plume footprints at different distances within the 80 kilometres of complex terrain surrounding the power plant (section 4). Finally, we recall the main results of the seasonal comparison of the SO<sub>2</sub> plume footprint within the study area (section 5).

## 2. METHODOLOGY

In this paper we compare the simulated and measured plume footprints found during two 3-day field campaigns. The first field campaign, during the summer of 1995, took place on 25, 26 and 27 July, and it has been selected as representative of the most recurrent summer scenarios (thermal mesoscale circulations, Palau 2003). The winter campaign took place on 26, 27 and 28 November 2001, and it has been selected as representative of the most recurrent winter scenarios in the area (winter Northwest advection; Palau, 2003). The climatological representativity of both meteorological scenarios has already been justified and published (Palau 2003; Palau et al. 2004b; Palau et al., 2006).

Systematic SO<sub>2</sub> surface measurements were carried out for these campaigns by the Regional Air Quality Network (continuously measuring air pollutants and meteorological parameters at different fixed locations around the power plant) and ENDESA (the power-generating company that owns this power plant).

The spatial density of the Air Quality Networks (figure 1) is not sufficient to perform a detailed evaluation of the simulated ground-impact areas in this complex terrain area (in spite of the temporal resolution of the measurements, recorded every 15 minutes). Nevertheless, the availability of continuous SO<sub>2</sub>-concentration measurements at the available sites, enabled the quantification of spatial biases between the measurements within the study area and the simulated ground-concentration field during the whole period considered. Thus, it was possible to analyse the seasonal differences in the SO<sub>2</sub>-plume footprint measured around the power plant within a complex terrain area extending more than 80 kilometres around said power plant. In this way, we were able to both diminish the temporal variabilities (uncertainties) associated with complex terrain areas where the spatial representativity of monitoring sites can be of the order of a few hundreds of metres, and evaluate the representativity of the spatial distribution of the simulated concentrations.

To analyse the seasonal differences in the physical processes driving the ground impacts of the plume aloft on selected spatial areas within the study area (figure 1), we have compared the three-day ground-level SO<sub>2</sub>

accumulation during nocturnal and diurnal hours for both the summer and winter campaigns. These two periods of the day, correspond to the different simulated turbulent regimes in the lower layers of the troposphere for both meteorological scenarios: a) in wintertime, the meteorological model simulates ground nocturnal impacts under mechanically driven turbulence, and diurnal impacts under both mechanically driven turbulence and forced convection (Palau et al. 2006); (b) in summertime, diurnal impacts are associated with free convection, and nocturnal impacts with mechanically driven turbulence (Palau, 2003).

In the first field campaign, during the summer of 1995, the comparison is made in 3 different areas and at different distances from the APP (figure 1a): at less than 20 Km from the power plant (zone s1: comprising the fixed stations of Monagrega, Foz-Calanda, Alcorisa and Mas Matas); at around 30 Km (zone s2: comprising Torrevelilla, La Ginebrosa and La Cerollera); and at more than 40 Km (zone s3: comprising Morella and Vallibona).

Similarly, for the winter campaign (due to experimental data availability), the areas (stations) considered are (figure 1b): around 40 Km from the power plant (zone w1: comprising Morella and Zorita); between 50 and 60 Km from the stack (zone w2: comprising Coratxar and Vallibona); and around 80 km from the stack (zone w3: comprising St. Jordi).

Simulations were performed using a non-hydrostatic mesoscale meteorological model MM5 (Grell et. al. 1994) coupled to a Lagrangian Particle Dispersion (LPD) Model FLEXPART (Stohl 2005). The mesoscale model MM5 uses a nested-grid configuration with 5 domains (100x100 grids spaced at 108, 36, 12, 4 and 1.3 Km, respectively) centred over the power plant (more details about the model configuration in Pérez-Landa et al. 2002, Palau et al. 2006). The model predicts the wind components  $u$ ,  $v$  and  $w$  and the turbulence parameters. Four-dimensional data assimilation (Stauffer and Seaman, 1994) was applied to the mother domain nudging toward the gridded 2.5° resolution NCEP Reanalysis. The LPD model FLEXPART takes into account wind velocity variances and Lagrangian autocorrelations. The spread of the pollutant is simulated by the Langevin equation derived by Thomson for inhomogeneous and Gaussian turbulence under non-stationary conditions (McNider et al., 1998). Turbulence statistics are obtained by using the Hanna scheme with some modifications taken from Ryall and Maryon for convective conditions (Stohl and Seibert, 2001). The FLEXPART model incorporates a density correction term for Gaussian turbulence which takes into account the density decrease with height within the Planetary Boundary Layer (Stohl and Thomson, 1999).

In our simulations, we treated the buoyant plume of the power plant by releasing particles at an effective stack height of 450 metres above ground level (m.a.g.l.), at 700 m.a.g.l. and at another variable height calculated hourly with Briggs' equations (Briggs 1975). The particles were released randomly within a  $10 \times 10 \times 100 \text{ m}^3$  volume at the beginning of the test simulations. Then, simulated plume footprints were performed considering the aforementioned three emission schemes.

For the two field campaigns selected, a detailed validation of the skills of the aforementioned coupled system MM5+FLEXPART in the simulation of the plume atmospheric dispersion has already been published by Pérez-Landa et al. (2002) and by Palau et al. (2003; 2006). In these studies, a direct quantitative comparison was performed between the dispersion conditions simulated by the numerical system and the available measurements. As a result, it was found that the coupled MM5+FLEXPART is capable of both reproducing the most relevant dispersion features of an elevated plume and predicting the plume integral transport from the APP onto the surrounding complex terrain. For the winter campaign, comparison between experimental and simulated transversal dispersion showed an index of agreement (Willmott, 1981) between 80% and 90%, within distance ranges from 6 to 33 Km from the stack (Palau et al. 2006). For the summer campaign, simulations and measurements showed an index of agreement between 84% and 88%, within distances ranging from 6 to 20 Km from the stack (Palau, 2003).

As a continuation of these previous studies, in the present paper the seasonal differences detected between the simulated  $\text{SO}_2$  ground-level concentrations in both simulated campaigns are compared with the available experimental measurements.

### 3. METEOROLOGICAL CONDITIONS

The two meteorological scenarios considered correspond (a) to a typical summer dispersion scenario under strong convective conditions and (b) to a frequent winter advective scenario in this mid-latitude area. The summer campaign took place on 25, 26 and 27 July 1995 and the winter one on 26, 27 and 28 November 2001. In both cases, we distinguish the diurnal period (from 7:00 to 22:00 UTC) from the nocturnal period (from 22:00 to 7:00 UTC).

*a) Summer campaign:* on the first day, the meteorological situation was conditioned by the passage of a low-pressure system over the Cantabrian Sea. On the second day, when the Low migrated to the NE, a ridge of high pressure arrived at the Iberian Peninsula. On the last day, the High was centred over the Cantabrian Sea and a Thermal Low formed in the south of the Iberian Peninsula. Thus, the wind in the area of interest came from the SE during most of the first day until it changed to SW due to the passage of the Low to the East. On the second and third day, nocturnal drainage occurred during the night and the wind flow followed the Ebro valley direction (NW) to the Mediterranean Sea. During daytime conditions the situation favoured the development of thermally driven mesoscale processes on both days (Pérez-Landa et al. 2002).

*b) Winter campaign:* during this field campaign typical winter conditions were recorded, characterised by three main pressure systems: an Atlantic anticyclone extending over the Iberian Peninsula, a Low located over the North of the British Isles and another low pressure system located on the Western Mediterranean Sea. This synoptic configuration (Palau et al. 2006) drove cross-isobaric flows, advecting the plume aloft towards the SE of the power plant (almost parallel to the Ebro valley axis towards the Mediterranean Sea) and inhibiting the development of thermally-driven local circulations.

#### 4. RESULTS AND DISCUSSIONS

For each of the two 3-day campaigns considered (winter and summer), the accumulated SO<sub>2</sub> concentrations measured at the available monitoring sites show a marked spatial bias regarding the distances between each monitoring station and the power plant chimney (not shown). This spatial bias is also present when disaggregating the 72-hour accumulated SO<sub>2</sub> concentration at each station into the nocturnal and the diurnal contribution (figure 2).

From the different emission schemes simulated during the summer and the winter campaigns, we obtained three accumulated SO<sub>2</sub> ground concentration patterns showing different quantitative characteristics (figure 3). One evident feature is the inverse correlation between the emission scheme performed and the magnitude of the SO<sub>2</sub> ground-level concentrations simulated. In this sense, Briggs' emission scheme results in accumulated ground-level SO<sub>2</sub> concentrations one order of magnitude lower than those obtained by performing constant emission schemes at 450 and 700 m.a.g.l. Nevertheless, for both seasons and from a qualitative point of view, there are important similarities. During the simulated summer campaign, and regardless of the emission scheme performed, the model identifies two large zones around the power plant with the highest SO<sub>2</sub> ground-level concentrations: one within a 20 km radius of the stack, and the other about 75 km downwind from the chimney (leeward of the Northern Maestrazgo mountain range), figure 3. For the simulated winter campaign, there are no significant differences between the simulated plume footprints in the three different emission schemes performed. In this winter case, the simulated SO<sub>2</sub> ground-level concentrations are located significantly leeward of the Northeast Maestrazgo mountain range. In this sense, although mechanical effects driven by topography are stronger in the case of the 450 m-high emission scheme than in the other two cases, the spatial pattern of the simulated SO<sub>2</sub> plume footprints does not essentially change with respect to the emission scheme performed (figure 3).

Coinciding with the SO<sub>2</sub> plume footprints described (figure 3), the remaining dispersion parameters directly compared with measurements (horizontal diffusion during the campaigns and direction of the integral advection of the plume aloft) were broadly independent of the emission scheme employed (table 1, extracted from Pérez-Landa et al. 2002; Palau et al. 2006). Disaggregating the plume footprints into diurnal and nocturnal contributions, the following main footprint features were identified to be independent of the plume-rise scheme used.

Under summer conditions, during the diurnal hours (between 7:00 and 22:00 UTC), an isotropic ground-level concentration field is simulated within a circular area with a radius of 20 km around the power plant; i.e., under summer conditions plume fumigations near the chimney are essentially equiprobable all around the chimney (figure 4a). On the contrary, diurnal plume impacts far away from the chimney are mainly located on leeward areas and are due both to topographic effects associated with nocturnal plume transport (being integrally-advected under stable conditions) during the first hours of the day, and to transitional periods (Pérez-Landa et al. 2002), while mesoscale circulations break the nocturnal transport regime (Palau 2003). During the nocturnal hours (between 22:00 and 7:00 UTC), the simulated ground-impact pattern shows the preferred transport directions of the plume, with a clear NW component (in agreement with the nocturnal spreading along the Ebro valley). There are three zones of with larger impacts along this axis: two leeward of the Maestrazgo mountains (SE from the APP, Northeast from Coratxar station, figure 4) and the third, closer to the APP, in the mountainous zone of the Mas de las Matas dam (20 km SE from the APP, figure 4b).

Under winter conditions, during nocturnal hours, accumulated SO<sub>2</sub> ground-level concentrations show a strong bias toward areas leeward of the mountains, with no simulated impacts near the power plant (figure 4d). As a result, the closest simulated impacts are located 45 km away from the chimney. In contrast, during daytime, although the strongest simulated impacts are leeward of the mountains, significant accumulated

impacts are simulated in a wider area and closer to the chimney than for the nocturnal hours (figure 4c). The accumulated impact pattern shows a preferred plume-transport direction towards East-Southeast from the chimney because of the synoptic NW advective conditions.

Comparing the daily patterns of measured SO<sub>2</sub> concentrations on the selected areas with the simulated concentrations on the same areas (figure 5), it is encouraging to note that, in agreement with the experimental records, during the summer campaign and regardless of the plume-rise scheme used, the simulated diurnal SO<sub>2</sub> ground-level impacts are larger than the simulated nocturnal SO<sub>2</sub> impacts within spatial zones one and two. On the other hand, in spatial zone three, both the simulated and the measured SO<sub>2</sub> nocturnal concentrations prevail over the diurnal ones.

During the winter campaign, there is a discrepancy between the simulated and experimentally measured nocturnal vs. diurnal preponderance in spatial zone two (figure 5). This discrepancy is due to a direct impact of the plume on the Coratxar station (which is located at the top of a mountain, within the plume advection height) during the first hours of the 26<sup>th</sup>. At this site, a very intense plume impact was recorded on the 26<sup>th</sup> during the nocturnal hours (maximum 1-hour average value of 1638 µg/m<sup>3</sup>, not shown). These extremely high SO<sub>2</sub> concentration values, together with the low wind speed measured (not shown), indicate that this plume impact was not associated with mechanical turbulence but rather with a direct plume impact on this site (for more details, Palau et al. 2006). Under stable conditions, the plume can be integrally advected as a ribbon-type plume (Millán, 1987), travelling long distances with very little vertical diffusion. This kind of impact (given its local nature) cannot be considered representative of the all of zone two, and it is difficult to simulate because of both the complexity of the topography and the very small spatial extension of the impact (associated with low dispersion conditions). Under such dispersion conditions, slight deviations between the real and the simulated plume advective direction have a strong impact when comparing simulated and measured local ground-level concentrations (and this limitation worsens even more on complex terrain). Nevertheless, the results obtained show how simulated mechanical turbulence leeward of the mountains reproduces highly concentrated SO<sub>2</sub> fumigations on the ground more than 60 kilometres away from the power plant, reproducing this observed feature qualitatively.

## 5. CONCLUSIONS

Two markedly different SO<sub>2</sub> ground-level distributions around the power plant are presented for typical summer and winter dispersion scenarios in the area. Measurements show that the SO<sub>2</sub> footprint of a plume being advected more than 450 metres above ground level in complex terrain is highly dependent on the prevailing meteorological conditions. Consistent with these observations, numerical simulations reproduce both the winter/summer mesoscale perturbations in the synoptic flows within the lower layers of the troposphere and the plume footprint around the power plant for both dispersion conditions.

Modelling and experimental results are in good agreement and show that under summer conditions the main features related to ground-level concentrations are: (a) during the diurnal hours, ground impacts near the source (<30km) due to convective activity; (b) during the night, ground impacts produced on the leeward side of mountains far away from the chimney (>40km). Features under winter conditions are: (a) plume impacts on the ground are produced near the source due to diurnal convective turbulence; (b) impacts far away from the chimney (>80 km) are driven by topographic effects and produced throughout the day.

Despite the model resolution, on complex terrain and under stable dispersion conditions (plume advected as a ribbon-type plume), limitations on the model performance have been evidenced due to the local nature of plume impacts far away from the chimney (>50 km). Under such dispersion conditions slight deviations between the real and the simulated plume advective direction have a strong impact when comparing simulated and measured local ground-level concentrations. Nevertheless, the results obtained show how on complex terrain, despite seasonal meteorological differences and under stable dispersion conditions, simulated mechanical turbulence leeward of the mountains reproduces highly concentrated SO<sub>2</sub> fumigations on the ground more than 60 kilometres away from the power plant. Besides, under summer convective activity, plume fumigations have been successfully simulated less than 15 kilometres from the power plant.

In conclusion, using an adequate high-resolution configuration of two models (MM5 and FLEXPART), it is possible to characterise seasonal SO<sub>2</sub>-plume footprint differences of an elevated plume in complex terrain under two recurrent dispersion scenarios associated with different topographically-fed meso-scale forcings. This numerical system has been able to identify hot spots in a semi-arid complex terrain region where information provided exclusively by fixed ground-level monitoring stations for atmospheric pollutant control could be insufficient and provide poor spatial significance.

Numerical models represent a clear advantage due to their spatial and temporal consistency which, combined with ground-level monitoring stations, can give a broad picture of the air quality in a particular region. As deduced from the results presented in this paper, detailed interpretation of simulated results (especially in

complex-terrain areas) can provide an added value for air quality management and air-quality network optimisation because models can identify hot spots where high air pollutant concentrations may be reached under specific meteorological conditions.

## 6. ACKNOWLEDGEMENTS

The CEAM Foundation is supported by the Generalitat Valenciana (Spain) and BANCAIXA. Moreover, this study has been jointly funded by the Conselleria de Cultura - "MEDICO" Project -- GV04B-069; by the Conselleria de Territori i Habitatge and Ciencia, and by the Ministerio de Ciencia y Tecnología, research projects "TRANSREG" (CGL2007-65359/CLI) and "GRACCIE" (CSD2007-00067, Programa CONSOLIDER-INGENIO 2010)". The authors would like to acknowledge all the people from the Fundación CEAM who participated in the field measurement campaigns.

## 7. REFERENCES

- Briggs, A. (1975) Plume rise predictions. In: Lectures on Air Pollution and Environment Impact Analysis. AMS, Boston (USA).
- COST 710 (1998) Harmonisation of the pre-processing of meteorological data for atmospheric dispersion models. COST Action 710 – Final report. European Commission. Directorate-General Science, Research and Development. EUR 18195 EN.
- Fast, J. D. (1995) Mesoscale modeling in areas of highly complex terrain employing a four-dimensional data assimilation technique. *J. App. Met.*, **34**, 2762-2782.
- Fast, J. D. and Darby, L. S. (2004) An evaluation of mesoscale model predictions of down-valley and canyon flows and their consequences using doppler lidar measurements during VTMX 2000. *J. App. Met.*, **43**, 420-436.
- Fast, J.D., Lance O'Steen, B. and Addis, R.P. (1995) Advanced atmospheric modeling for emergency response. *J. App. Met.*, **34**, 626-649.
- Grell, G.A., Dudhia, J. and Stauffer, D.R. (1995) A description of the fifth-generation Penn State/NCAR mesoscale model (MM5). NCAR/TN-398+STR, National Center for Atmospheric Research, Boulder, CO (USA), 138.
- McNider, R.T., Moran, M.D. and Pielke, R.A. (1998) Influence of diurnal and inertial boundary-layer oscillations on long-range dispersion. *Atmos. Environ.*, **22** (11), 2445 – 2462.
- Millán M., Navazo M., Ezcurra, A., 1987. Meso-Meteorological analysis of air pollution cycles in Spain. *Physico-Chemical Behaviour of Atmospheric Pollutants*. G. Angeletti and G. Restelli, Editors. D. Reidel Publishing Co. Dordrecht, Holland. For the Commission of the European Communities, pp 614-626.
- Millán M.M., Sanz M.J., Calatayud V., Palau J.L., Diéguez, J.J., Pérez-Landa G., Mantilla E., Cerveró J., Chordá, J.V. (2004) La calidad del aire en las comarcas de Els Ports-Maestrat (Air quality on the Els Ports-Maestrat areas). Edited in Spanish by Generalitat Valenciana (Conselleria de Territori i habitatge) and Fundación CEAM, 408, ISBN: 84-921259-4-2, Valencia (Spain).
- Millán, M. M., Artiñano, B, Alonso, L, Castro, M., Fernandez-Patier, R. and Goberna, J. (1992) Meso-Meteorological Cycles of Air Pollution in the Iberian Peninsula, (MECAPIP) (Air Pollution Research Report 44, EUR No. 14834). European Commission DG XII/E-1, Rue de la Loi, 200, B-140, Brussels.
- Millán, M.; Alonso, L.; Legarreta, J.A. (1986) Dispersión de contaminantes en la atmósfera: Parte I. (Atmospheric pollutants dispersion. Part I). In Spanish. *Energía*, julio-agosto, Madrid (Spain), 89-101.
- Millán, M.M. (1987) The regional transport of tall stack plumes. In: Sandroni, S. (ed.): *Regional and Long-range Transport of Air Pollution*. Elsevier Science Publishers, Amsterdam, The Netherlands, 249-280.
- Millán, M.M., Gallant, A.J. & Turner, H.E. (1976). The Application of Correlation Spectroscopy to the Study of Dispersion from Tall Stacks. *Atmospheric Environment*, **10**, 499-511.
- Palau J. L. (2003) Dispersión atmosférica de las emisiones de una chimenea alta en terreno complejo (Atmospheric dispersion of a tall-stack plume on complex terrain). PhD Thesis (in Spanish). University of Valencia (Spain). Edited by Fundación CEAM, 366, ISBN: 84-688-4440-3, Valencia (Spain).
- Palau J.L., Monter C., Millán M. M. (2004b) Influencia de la Baja Térmica Ibérica en la dinámica del penacho de una Chimenea Alta (Influence of the Iberian Thermal Low on the dynamics of a plume emitted from a tall chimney). In Spanish. *PROMA-Feria del Medio Ambiente: IX Congreso de Ingeniería Ambiental*, 521-530, Bilbao (Spain).
- Palau, J. L., Mantilla, E., Millán, M. M. (2001) Estimation of the dispersion of an elevated plume on complex terrain under stable-to-neutral conditions. A changing atmosphere: 8<sup>th</sup> European Symposium on the Physico-Chemical Behaviour of Atmospheric Pollutants. 17-20 September. Torino (Italy).
- Palau, J. L., Pérez-Landa, G., Diéguez, J. J., Monter, C., and Millán, M. M. (2005) The importance of meteorological scales to forecast air pollution scenarios on coastal complex terrain. *Atmos. Chem. Phys.*, **5**, 2771-2785. <http://www.atmos-chem-phys.net/5/2771/acp-5-2771-2005.pdf>
- Palau, J.L., Pérez-Landa, G., Meliá, J., Segarra, D., Millán, M.M. (2006) A study of dispersion in complex terrain under winter conditions using high-resolution mesoscale and Lagrangian particle models, *Atmos. Chem. Phys.*, **6**, 1105–1134. <http://www.atmos-chem-phys.net/6/1105/2006/acp-6-1105-2006.pdf>

- Palau, J.L., Pérez-Landa, G.; Meliá, J.; Segarra, D.; Millán, M.M. (2004a) A study of the dispersion of a power plant on complex terrain under winter conditions in the Iberian Peninsula. Fourth Annual Meeting of the European Meteorological Society. EMS Annual Meeting Abstracts, Vol. I, 00389. Nice (France).
- Perez-Landa, G.; Palau, J.L.; Mantilla, E.; Millán, M.M. (2002) A study of the dispersion of a power plant on complex terrain under summer conditions. 15<sup>th</sup> Conference on Boundary Layer and Turbulence. AMS, 346-349. Wageningen.
- Pooler, F. Jr. and Niemeyer, L.E. (1971) Dispersion from tall stacks: An Evaluation. Proceedings 2<sup>nd</sup> International Clean Air Congress (H.M. Englund and W.T. Beery editors), Academic Press, New York.
- Salvador, R.; Calbó, J. And Millán, M.M. (1999) Horizontal grid size selection and its influence on mesoscale model simulation. Journal of Applied Meteorology, **38** (9), 1311-1329.
- Shiermeier, F.S. (1971) Study of effluents from large power plants. Presented at the American Industrial Hygiene Assoc. Conf. May. 24-28, Toronto, Canada.
- Stauffer, D.R. and Seaman, N. L. (1994) Multiscale four-dimensional data assimilation. J. Appl. Meteor., **33**, 416 - 434.
- Stohl, A. and Seibert, P. (2001) The FLEXPART particle dispersion model. User Guide. <http://www.forst.uni-muenchen.de/EXT/LST/METEO/stohl/>
- Stohl, A. and Thomson, D. J. (1999) A density correction for lagrangian particle dispersion models. Boundary-Layer Meteorology, **90**, 155-167.
- Stohl, A., Forster, C., Frank, A., Seibert, P., Wotawa, G. (2005) Technical note: The Lagrangian particle dispersion model FLEXPART version 6.2. Atmos. Chem. Phys., **5**, 2461-2474.
- Willmott, C. J. (1981) On the validation of models. Physical Geography, **2**(2), 184-194.
- Zaremba, L. L. and Carroll, J. J. (1999) Summer wind flow regimes over the Sacramento valley. J. App. Met., **38**, 1463-1473.

Field Campaign	Day/ Month	Hour Begin.	Hour End.	Distance (km)	Experimental Dispersion (km)	Simulated dispersion Briggs (km)	Simulated dispersion 700m (km)	Simulated dispersion 450m (km)
WINTER								
	26/11	10:45	11:58	26.68	3.03	1.70	1.33	3.18
	26/11	13:21	14:12	20.57	1.14	1.64	1.40	1.29
	26/11	15:12	15:35	15.79	2.49	1.59	1.05	1.75
	26/11	16:01	16:16	12.33	1.02	0.55	0.90	2.01
	27/07	08:35	09:45	8.04	0.94	0.40	0.25	0.34
	27/07	09:45	10:25	13.02	1.69	1.22	0.50	1.03
	27/07	11:03	13:15	32.78	2.45	2.19	1.63	2.14
	27/07	14:23	15:04	6.87	0.58	0.76	0.84	0.73
	27/07	15:06	15:40	14.99	1.05	1.74	1.85	1.90
	27/07	15:41	16:09	6.40	0.86	0.50	0.69	0.81
	28/11	08:17	09:54	19.84	1.00	0.83	0.56	0.74
	28/11	09:55	11:00	6.18	0.85	0.00	0.00	0.50
	28/11	11:01	11:56	7.41	1.54	0.84	0.50	0.73
	28/11	11:57	13:09	6.33	1.13	1.01	0.93	0.84
	28/11	14:16	14:44	6.31	0.93	0.50	0.49	0.87
SUMMER								
	25/07	09:50	11:30	6.07	0.79	1.31	1.24	1.16
	25/07	16:17	16:54	15.49	0.92	2.79	3.05	2.55
	26/07	07:15	08:49	9.97	1.89	1.24	1.30	0.95
	26/07	08:57	09:17	9.94	1.96	2.38	2.19	1.77
	26/07	09:25	10:06	19.14	4.63	5.48	5.58	5.27

**Table 1.** Summary of values of the dispersive results for the two field campaigns (extract from Pérez-Landa et al. 2002, Palau et al. 2006). Hour begin: Starting time of the measurements (in UTC); hour end: Finishing time of the measurements (in UTC); Distance: Distance to the stack; Experimental dispersion:  $\sigma_y$  of the plume aloft.

<b>WINTER DAY/NIGHT PERCENTUAL VARIATION OF SO<sub>2</sub> GROUND-LEVEL CONCENTRATIONS</b>				
	Experimental	Emission 450 m	Emission 700 m	Briggs emission Scheme
ZONE w1	57.7	100.0	100.0	100.0
ZONE w2	-113.1	90.6	85.4	80.9
ZONE w3	-122.6	-295.8	-92.2	-796.4

<b>SUMMER DAY/NIGHT PERCENTUAL VARIATION OF SO<sub>2</sub> GROUND-LEVEL CONCENTRATIONS</b>				
	Experimental	Emission 450 m	Emission 700 m	Briggs emission Scheme
ZONE s1	85.9	-5.3	87.0	16.7
ZONE s2	38.8	49.4	87.6	58.9
ZONE s3	-305.6	-135.0	330.0	-690.0

Table 2. Seasonal “day/night” percentual variation in the mean ground-level SO<sub>2</sub> concentrations throughout the field campaigns at three different areas Southeast from the APP. Positive variations indicate that diurnal impacts prevail; negative variations indicate that nocturnal impacts prevail. Values are expressed in % and are calculated from  $100 \times ([SO_2]_{day} - [SO_2]_{night}) / [SO_2]_{day}$ . This table is related to figure 5. Data extracted from Palau, 2003 and Palau et al. 2006.

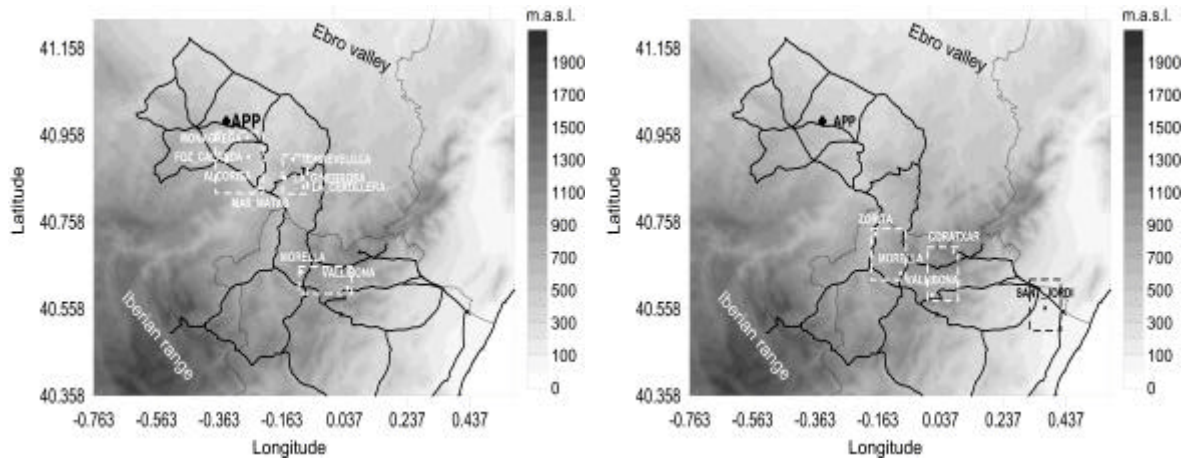


Figure 1: Study area around the Andorra Power Plant (APP) in the North-East of the Iberian Peninsula, near the Mediterranean sea. Light-black lines indicate borders of three Spanish provinces and black lines the available road network around the APP. Left (a), summer campaign; Locations of the nine available air quality stations are labelled. Squares indicate the three different orographic areas where plume impacts on the ground were analysed by comparing the simulated results with measurements. Altitudes are indicated in metres above sea level (m.a.s.l.). Right (b), winter campaign: Locations of the five available air quality stations are labelled. Squares indicate the three different orographic areas where plume impacts on the ground were analysed by comparing the simulated results with measurements.

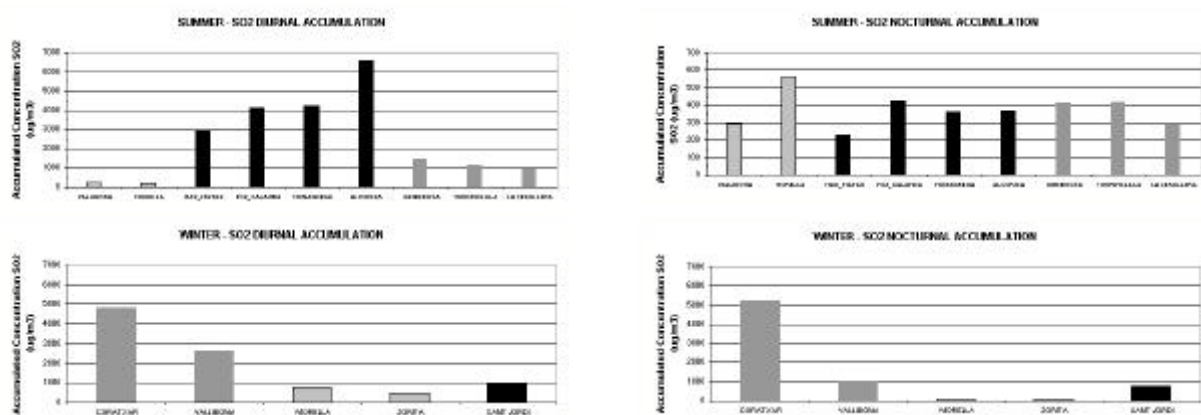


Figure 2. Accumulated concentration of SO<sub>2</sub> (during the diurnal and nocturnal hours) for the different stations during the summer and the winter campaigns.

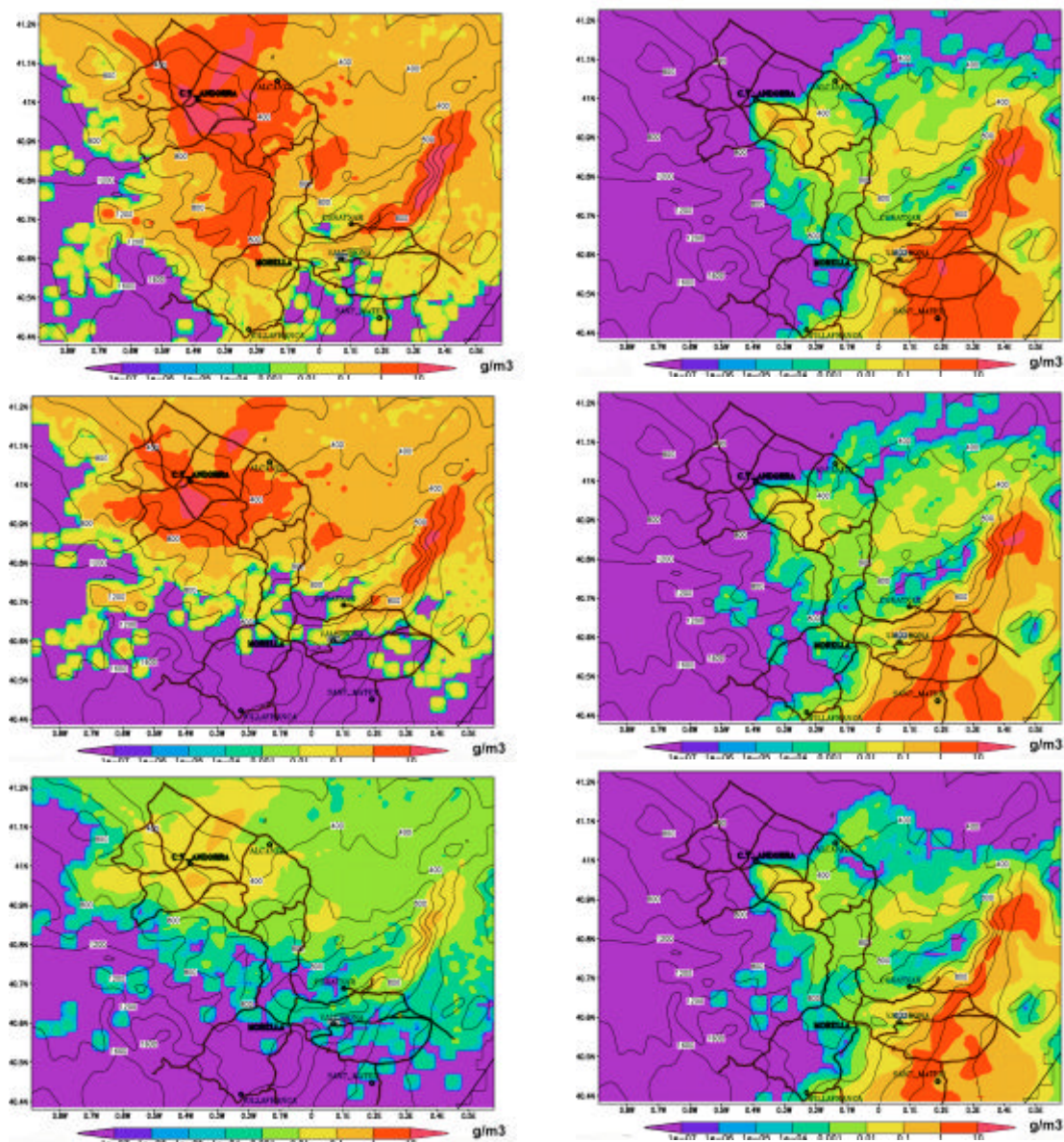


Figure 3: Simulated impact patterns for the three emission schemes. Left column corresponds to the summer campaign and right column to the the winter campaign: 450m scheme (top-left A and top-right B), 700m scheme (middle-left C and middle-right D) and Briggs' scheme (bottom-left E and bottom-right F).

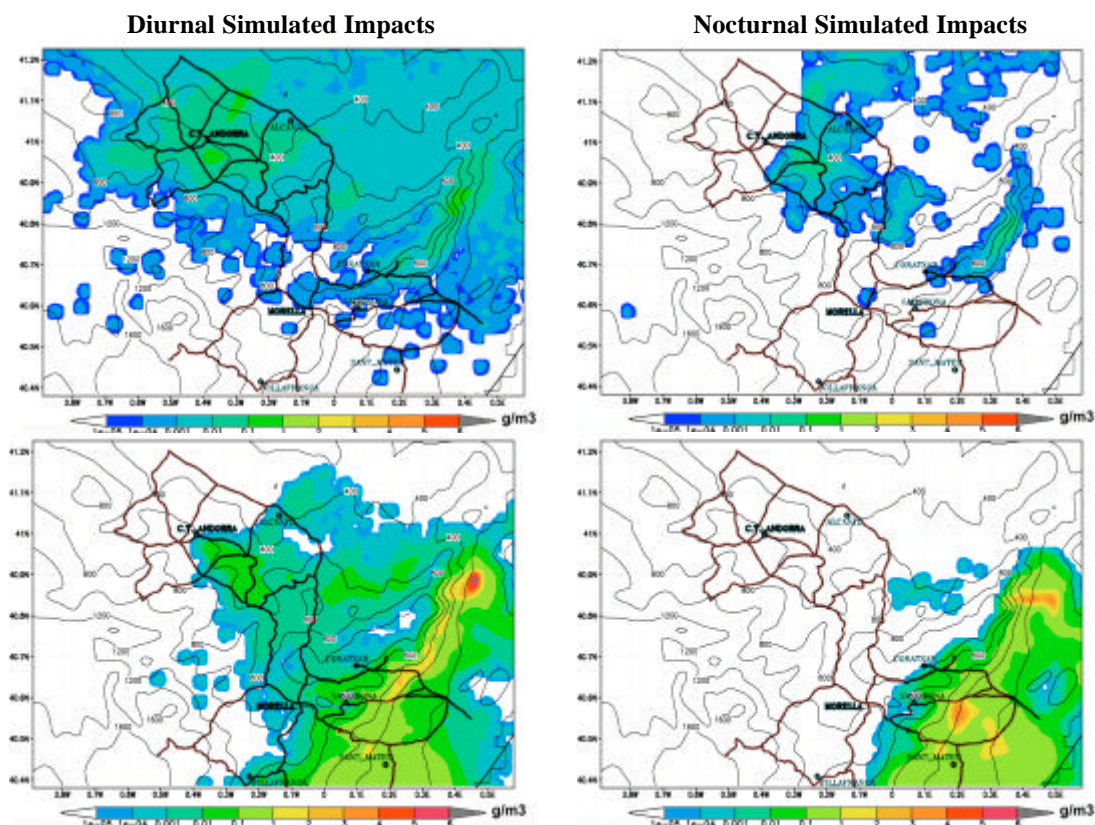


Figure 4: simulated impact patterns for the diurnal-nocturnal hours. By rows, summer (top a, b) and winter (bottom c, d) periods, respectively.

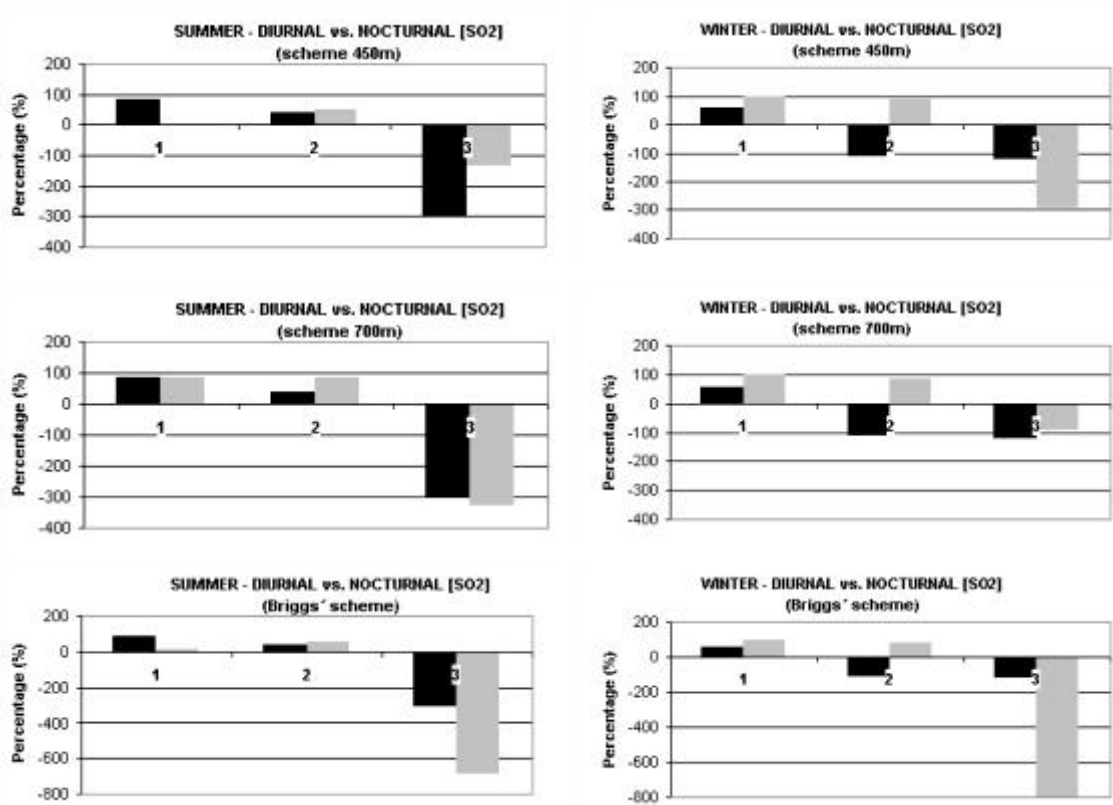


Figure 5. Diurnal vs. nocturnal concentrations (percentage) calculated for the 3 different plume-rise schemes during the summer and winter campaigns (greater than zero indicates that diurnal impacts are greater than nocturnal impacts). Black squares: measurements; grey squares: simulated results.